Applying Advanced Technologies in Support of Landscape Restoration and Climate Change Adaptation

Investing in Climate Change Adaptation through Agroecological Landscape Restoration: A Nature-Based Solution for Climate Resilience (Technical Assistance 6539)

October 2023

Dontret, Cambodia (photo by ICEM)

ADB

JFPR
Japan Fund for Prosperous and Resilient Asia and the Pacific

From the People of Japan

icem

World Agroforestry

Disclaimer

This document was prepared for the Asian Development Bank (ADB) by a joint venture of the International Centre for Environmental Management (ICEM) and World Agroforestry (ICRAF). The views, conclusions, and recommendations in this document are not to be taken to represent the views of ADB.

Prepared by	ICEM and ICRAF
Prepared for	ADB
Suggested citation	ICEM & ICRAF. 2023. *Applying Advanced Technologies in Support of Landscape Restoration and Climate Change Adaptation (Knowledge Product 7)*. Investing in Climate Change Adaptation through Agroecological Landscape Restoration: A Nature-Based Solution for Climate Resilience (Technical Assistance 6539). Prepared for Asian Development Bank. Hanoi.
Deliverable summaries	TA-6539 Investing in Climate Change Adaptation through Agroecological Landscape Restoration: A Nature-Based Solution for Climate Resilience led to the preparation of the following knowledge products:

- KP1 (1): Landscape Restoration Country Profile: Philippines
- KP1 (2): Landscape Restoration Country Profile: Cambodia
- KP3: Business Models to Encourage Private Sector Participation in Sustainable Land and Forest Landscape Management
- KP4 (1): Climate Change Risk and Adaptation Options Assessment – Sangker River Basin, Cambodia
- KP4 (2): Climate Change Risk and Adaptation Options Assessment – Manupali Watershed, Mindanao River Basin, the Philippines
- KP5: Good Practices Manual on Biodiverse Forest and Landscape Restoration
- KP6: Community-based Climate Vulnerability Assessment and Adaptation Planning for Resilient Agroecosystems
- KP7: Applying Advanced Technologies in Support of Landscape Restoration and Climate Change Adaptation
- KP8 (1): User Manual: Sangker River Basin Decision Support System
- KP8 (2): User Manual: Mindanao/Manupali River Basin Decision Support System
- KP8 (3): Admin Manual: Sangker River Basin Decision Support System
- KP8 (4): Admin Manual: Mindanao/Manupali River Basin Decision Support System
- KP9 (1): Restoration plans for demonstration areas in Cambodia and the Philippines
- KP9 (2): Gender and Social Inclusion in the Mindanao River Basin, the Philippines, and the Sangker River Basin, Cambodia
- KP10: Integrating the principles of ecological agriculture into upland farming systems of Manupali Watershed, the Philippines

Project Team	**ICEM-ICRAF** Jeremy Carew-Reid, Caroline Duque-Pinon, Enrique Lucas Tolentino, Jr., Khun Bunnath, Heng Bauran, Jago Penrose, Lay Chanthy, Michael Waters, Mark Hopkins, Nguyen Bich Ngoc, Nguyen Phuong Thao, Orlando Fernando Balderama, Paulo Pasicolan, Porny You, Quang Phung, Rachmat Mulia, Richard Cooper, Trond Norheim, Zarrel Gel M. Noza
Photo credit	Cover page: Dontret. Cambodia (photo by ICEM) Back page: Anakut Koma Samaki, Cambodia (photo by ICEM)

CONTENTS

Figures

Tables

Abbreviations

ACD	Above-ground Carbon Density
AGB	Above ground biomass
ALOS	Advanced Land Observing Satellite
ARSET	Applied Remote Sensing Training Program
ESA	European Space Agency
ESRI	Environmental Systems Research Institute
EVI	Enhanced Vegetation Index
GEE	Google Earth Engine
GFW	Global Forest Watch
ISRIC	International Soil Reference and Information Centre
ISRO	Indian Space Research Organization
JAXA	Japan Aerospace Exploration Agency
K-NN	K-Nearest-Neighbor
LiDAR	Light Detecting and Ranging
MODIS	Moderate Resolution Imaging Spectroradiometer
MRV	Measurement, Reporting and Verification
NASA	National Aeronautics and Space Administration
NDVI	Normal Different Vegetation Index
NISAR	NASA-ISRO Synthetic Aperture Radar
PEN	Phenological Eyes Network
SAR	Synthetic Aperture Radar
PALSAR	Phased-Array L-band Synthetic Aperture Radar
RADAR	Radio Detection And Ranging
REDD	Reducing Emissions from Deforestation and Forest Degradation
TSL	Terrestrial Laser Scanners
WRI	World Resources Institute
UAV	Unmanned Ariel Vehicle
UNSPIDER	United Nations Platform for Space-based Information for Disaster Management and Emergency Response
UMD	University of Maryland

Acknowledgements

In Cambodia, the *Technical Assistance (TA) 6539: Investing in Climate Change Adaptation through Agroecological Landscape Restoration: A Nature-Based Solution for Climate Resilience Project* was led by the Ministry of Environment (MOE) under the continuing direction and guidance of His Excellency Khieu Borin, Under-Secretary of State and His Excellency Chuop Paris, Secretary of State. MOE staff who have provided important technical inputs to the project are Mr. Kamal Uy, Ms. Chanthyda Meas, and Mr. Lihuor Phady. A special thanks to Mr. Sokunwath Phat, the MOE liaison officer to the project, and Mr. Samey Ly, the Samlaut Multiple Use Area Director, Battambang Province and Mr. Ra Eav the SMUA Park Director, Pailin Province. Local Government staff who contributed significantly include Mr. Seng Samay, Forest Administration Officer; Mr. Chloem Loo, Border Police Officer; MOE Rangers Mr. Sophy Chim, Ms. Channoun Om, Mr. Sarith Yong, Mr. Heng Chhay, Mr. Yoeung Pov, Mr. Thou Pov, Ms. Chreb Eav, Mr. Sophea Toeung, Mr. Mao Sopheak, Mr. Vuthy Em, Mr. Veasna Men, Mr. Thom Boy and Mr. Sarat Pem; and Gendarmes Mr. Kheng Sok and Mr. Chet Heng.

In the Philippines the project was led by the River Basin Control Office of the Department of Environment and Natural Resources under the close direction and support of RBCO Executive Director Nelson Gorospe. The project also received the invaluable support of Edward Dominic Valencia, the Project Coordinator for Mindanao between 2020 and 2022 and Christian Libang, Technical Assistant and Project Coordinator for Mindanao from 2023.

Members of the DENR Technical Working Group set up to review all project outputs were Felix Mirasol, Jr., DENR Region 10; Ali Hadjinasser, DENR Region 12; Conrado Bravante, Jr., Foreign-Assisted and Special Projects Service; Imelda Matubis, Climate Change Service; Ma. Teresa Aquino, Forest Management Bureau; Anson Tagtag, Biodiversity Management Bureau, and Nathan Tambobong, National Water Resources Board.

Local Government and non-government representatives who actively participated in the many field activities and events and provided inputs to project documentation were Ms. Cecille Egnar, Bukidnon Environment and Natural Resources Officer; Dr. Joy Mirasol President of Bukidnon State University; Dr. Lesley Lubos, Research Director at Bukidnon State University; Ms. Vivien Belderol-Necosia, Instructor at Bukidnon State University; For. Conrado Marquez, Assistant Director at DENR-Ecosystems Research and Development Bureau; Ms. Lydia Tiongco, Senior Science Research Specialist, FWRDEC; Mr. Vergilino Alima, Provincial Environment and Natural Resources Officer, Bukidnon; Ms. Merlita Luna-Tabamo, Protected Area Superintendent (DENR), Mt. Kitanglad Range Natural Park; Hon. Ernie Debivar, Mayor and Local Chief Executive, Municipality of Lantapan, Bukidnon; Mr. Leonard Hope Labial Environmental Management Officer, Municipal Environment and Natural Resources Office MENRO-Lantapan; Mr. Recto Canda, at MENRO-Lantapan; Mr. Nephtali Ambos Municipal Agriculturist, Municipal Agriculturist's Office; Ms. Nonilita Butaya, Municipal Tourism Officer, Municipal Tourism Office; Hon. Boycon Empaguey, Chairperson Barangay Local Government Unit of Songo, Lantapan; Hon. Jieve Gamay, Councilor and Committee Head for Agriculture and Environment Barangay, Local Government Unit of Songo, Lantapan.

Ms. Sugar Gonzales of the ADB Sustainable Development & Climate Change Department provided overall management of the project and strong technical and operational inputs throughout, supported by Ms. Dianne Delfino. Mr. Alvin Lopez of ADB's Southeast Asia Department also contributed significantly to activities and outputs of the project.

Most important, the project and its knowledge products would not have been so effective without the commitment and engagement of more than one hundred farmers in Cambodia's Sangker River headwaters and in the Manupali watershed within the Mindanao River Basin of the Philippines. Their work in restoring degraded areas in and around their farms was the source of inspiration and lessons for the various knowledge products arising from the project – and to the sustainability of project initiatives and impacts.

1 Introduction

Forest landscape restoration is increasingly a high-technology, data-intensive process. The Global Partnership on Forest Landscape Restoration defines forest landscape restoration as: "an active process that brings people together to identify, negotiate and implement practices that restore an agreed optimal balance of the ecological, social and economic benefits of forests and trees within a broader pattern of land uses".[1] Technology now contributes and facilitates every stage of the forest restoration process[2], from identifying degraded sites and corridors and providing baselines to monitor spatial and temporal changes in habitats, to identifying species and even collecting and planting seeds.

Remote sensing technologies can provide an extensive range of information about sites and whole forests. Particularly when used in combination remote sensing technologies can determine tree dimensions, forest types, crown density, basal cover, above-ground biomass (AGB), the presence and mass of deadwood, the extent and nature of forest canopies, vegetation and even species composition above and below the forest canopy. This information can, in turn, be used to determine the carbon stored in the biomass, the extent of biodiversity, structural complexity, and where the forest is on the spectrum between degraded and the reference, or restored state.[3]

There is no one optimal remote sensing technology. Choices between technologies, whether platform, sensor or software, will often involve trade-offs and depend on financial and technological constraints and the nature of the study at hand.

Platforms are typically presented as a choice between spaceborne, airborne, and ground-based. However, there is substantial variation within each broad category. As Section 2 sets out, the range of satellites available is increasing all the time, each offering different services. Although historically including helicopters and planes, airborne services have largely become redundant, giving way to high-resolution satellite imagery and unmanned ariel vehicles (UAVs). Here too, as Section 3 makes clear, choices depend on cost, distance, sensors, and availability. Ground-based platforms include cameras, mobile phones, and sensors. However, in many respects, the "system is the sensor," and comprehensive results often depend on how various platforms complement each other and are combined.

Sensors are critical to remote sensing, and the choice of sensor is again dependent on cost, availability, and need. Spaceborne and Airborne Sensors collect signals reflected from the earth, and can be organized into active sensors - in which the sensor sends and receives a signal (for example, RADAR and Light Detecting and Ranging (LiDAR)), and passive sensors, whereby the sensor collects signals naturally transmitted from the earth's surface. Section 4 will illustrate that sensors are suited to different uses, and often demand trade-offs, depending on the study's spatial (global to local) and temporal (daily to yearly) scale and questions asked.

Increasingly the choice of technology must consider the software, computing power, and expertise available to interpret results. Sensors, whether mounted on satellites, drones, handheld devices, or living trees, collect data that requires interpretation and communication.

As computing power increases and becomes more available, the ability to interpret subtle differences in signals at the level of a single pixel amongst millions opens up opportunities, even for data collected in the recent past. Section 6 will introduce some of the main approaches to data collection and interpretation and, again, point to the benefits of combining sensors, technologies, and platforms.

[1] https://www.forestlandscaperestoration.org/
[2] Camarretta, P. A. (2020). Monitoring forest structure to guide adaptive management of forest restoration: a review of remote sensing approaches. _New Forests_, 573–596
[3] Pandey, C. and Arellano, P. 2023. Advances in Remote Sensing for Forest Monitoring, First Edition. John Wiley and Sons Ltd.

2 From Space: Satellites

From the first Landsat mission in 1972 and the launch of the first commercial satellite systems in 1999, the role of satellites has advanced significantly. Moreover, the usefulness of the data and images collected by satellites has increased at arguably a faster rate as the knowledge collected has been made freely available, as have the tools and computing power to interpret it. Although the costs of launching satellites is prohibitive to most, the costs of accessing satellite output have fallen almost to zero, putting the onus on the analyst to find new ways of harnessing a rapidly increasing amount of information, and communicating it effectively to resource managers.

Satellite imagery confers a range of benefits and will suffice for most uses. Satellites carry different sensors and combinations of sensors (see Section 4), producing a range of types of imagery. As such, information extracted from satellite images can provide the basis for much of the analysis required. Section 7.3 offers a practical example of using satellite imagery to monitor changes in land cover in Cambodia.

The regularity of images is also increasing. Historically satellites would take consistent measurements at specific time intervals, depending on orbits. Landsat, for example, would revisit the same spot every 16 days.[4] Improved technology, however, means that some commercial satellites can focus on specific areas for prolonged periods. As they orbit the earth, newer generations of satellites can focus on particular points for long periods. When used as a "constellation," the burden can be shared, reducing the time between visits (e.g. Sentinel). A recent survey of the use of remote sensing technologies found that Landsat has proved to have particular advantages over other systems, not least its status as the longest uninterrupted earth observation program and the first to offer free images. Nevertheless, as the same study indicates, rival systems such as Sentinel 2 and RapidEye will provide similar long-term quality imagery over the next decade or so.[5]

The low cost, consistency, geographic scale, and range of satellite data grant satellite imagery significant advantages over UAVs. However, the image resolution tends to be coarser than lower-level sensors and less suitable for detailed measurements of smaller areas, although this is changing with newer generations of satellites. Satellite observations are also determined by "temporal resolution" or revisit times, potentially limiting the opportunity to make immediate or regular observations. Satellites may also be limited to particular territories at particular times. As high resolution sensors tend to take longer to cover a target area there also tends to be a trade-off between temporal and spatial solutions. Even so, technological advances, including the availability of higher resolutions mean that satellite imagery is increasingly considered a valid alternative.

2.1 Satellites

New generations of satellites carry increasingly sensitive sensors, opening up possibilities for forest and biodiversity assessment monitoring. For example, improved sensors in Landsat 8 and 9[6] have increased vegetation sensitivity[7], enabling more precise detection and analysis of above-ground biomass and carbon.[8] Similarly, the three red edge bands included in Sentinal 2 also improve biomass

[4] Lechner, M. et al. 2020. Applications in Remote Sensing to Forest Ecology and Management. One Earth. Accessed here: https://core.ac.uk/reader/328760320

[5] Gyamfi-Ampadu, E. and Gebreslasie, M. 2021. Two Decades Progress on the Application of Remote Sensing for Monitoring Tropical and Sub-Tropical Natural Forests: A Review. Forests 2021, 12, 739. https://doi.org/10.3390/ f12060739

[6] Landsat 9. 2021. Webpage, accessed here; https://landsat.gsfc.nasa.gov/satellites/landsat-9/

[7] Roy, D.P. et al. 2014. Landsat-8: Science and product vision for terrestrial global change research. Remote Sens. Environ. 2014, 145, 154–172.

[8] Gyamfi-Ampadu, E. and Gebreslasie, M. 2021. Two Decades Progress on the Application of Remote Sensing for Monitoring Tropical and Sub-Tropical Natural Forests: A Review. Forests 2021, 12, 739. https://doi.org/10.3390/ f12060739

and carbon estimates.[9] This improved performance, coupled with comprehensive coverage and low costs to users, has resulted in a rapid increase in the use of both systems in the last few years.[10]

2.2 Available Satellites

Analysts have access to imagery from a growing range of satellites. Originally, operating in isolation, satellites now often form "constellations", which can increase the regularity of coverage and the combination of technologies employed. New satellites are also scheduled for launch, with new, more sophisticated sensors on board such as ALOS-3 and NASA-ISRO Synthetic Aperture Radar (NISAR) that will provide detailed images at greater frequencies (Table 2.1). NISAR, for example, will provide biweekly observations of 90% of each of the world's forests using both standard S-bands and L-bands (see Section 4.3), able to penetrate canopy, and so provide estimates of forest volume and biomass over time.[11]

Table 2.1: Remote Sensing Satellites, Planned and In Operation

Accessibility	Satellite/Sensor name	Year launched	Number of bands or polarizations	Resolution	Revisit time/day
Open	Landsat 9	2021	11	30m, 15m, 100m	16
Open	Landsat 8	2013	11	30m, 15m, 100m	16
Open	Landsat 7	1999	8	30m, 15m, 60m	16
Open	Sentinel-2 (A and B)	2015	13	10m, 20m, 60m	5
Open	Sentinel-1	2014	VV, HV, HH, VH	10m	12
Open	MODIS	1999	36	250m, 500m, 1000m	1-2
Open and commercial	ALOS2/PALSAR-2	2014	HH, HV, VH, VV	0.625m - 100m	
Commercial	WorldView-3	2014	29	1.24	1–4.5
Commercial	WorldView-4	2016	5	1.24	1–4.5
Commercial	Pléiades-1A and 1B	2011	5	2	1
Commercial	RADARSAT-2	2007	VV, HV, HH, VH	3-100m	24
Open	NISAR	To be launched in 2024	L-band, S-band HH, HV, VH, VV	3-10m	12
Open and commercial	ALOS-3	Launched February 2023.	7	2.8m, 3.2m	35

[9] Gyamfi-Ampadu, E. and Gebreslasie, M. 2021. Two Decades Progress on the Application of Remote Sensing for Monitoring Tropical and Sub-Tropical Natural Forests: A Review. Forests 2021, 12, 739. https://doi.org/10.3390/ f12060739
[10] Gyamfi-Ampadu, E. and Gebreslasie, M. 2021. Two Decades Progress on the Application of Remote Sensing for Monitoring Tropical and Sub-Tropical Natural Forests: A Review. Forests 2021, 12, 739. https://doi.org/10.3390/ f12060739
[11] NASA. 2022. Monitoring Global Forest Resources. NASA. Accessed here: https://nisar.jpl.nasa.gov/documents/16/NISAR_Applications_Forest_Resources1.pdf

3 Airborne Technologies

Airborne technologies include airplanes, helicopters, and UAVs. As technology progresses, battery life improves, and UAVs become increasingly affordable, UAVs are the tool of choice for more localized studies. UAVs can be fixed or rotor wing. They differ in terms of size, payloads, range, and battery power. Table 3.1 provides a summary of commonly used UAVs and manned aircraft.

Table 3.1: Specifications of Some Small Unmanned Ariel Vehicles and Manned Aircrafts in Forest Monitoring

Platform name	System type	Sensor type and name	Forest applications	Source
DJI M600 Pro	Rotary wing	Lidar: RIEGL miniVUX-1 UAV	Tree height	(Chen, 2022)
DJI Phantom 4 Pro	Rotary wing	RGB	Aboveground biomass	(Swayze, 2022)
DJI Matrice 600 Pro	Rotary wing	Velodyne VLP-32c LiDAR	Stem volume, tree DBH, tree height, aboveground biomass	(Dalla Corte, 2022)
DJI Phantom 4 RTK	Rotary wing	Complementary Metal-Oxide Semiconductor (CMOS) multispectral sensor	Pest infestation	(Xu, 2022)
Cessna 208 Caravan manned aircraft	Manned aircraft	Leica Geosystems TerrainMapper LiDAR sensor	Aboveground biomass	(Hantao Li, 2022)

The main advantages of drones and other UAVs are their mobility, relative cost, and, depending on payload, ability to utilize monitoring and sensor technologies and carry and collect data and even seeds. From a practical perspective, drones can access otherwise inaccessible sites on a regular basis, and their relative simplicity also means they can be easily operable with minimum levels of training. Drones, for example, are increasingly used as part of Community Based Forest Assessments[12] and other projects in which community members and lay people can support scientific or monitoring programs. As discussed below, limitations increasingly lie not in the access to or operation of drone technology but in the processing and interpretation of collected data.

3.1 Uses of Unmanned Ariel Vehicles

The effectiveness of UAVs in forest monitoring lies mainly in the sensors they carry, the information they can collect, and its post-processing and interpretation. Their relative proximity to the ground and the smaller study areas mean that drone cameras tend to take images at a higher resolution than satellite. When combined with appropriate software and sensors, UAVs can serve a number of uses:

- ***Site Surveys:*** Drones can undertake initial identification and surveys of interested sites. Combinations of camera technology and other sensors can help provide accurate survey site baselines.
- ***Site Monitoring*****:** In subsequent periods, drones can monitor the progress of restoration efforts and observe encroachments onto sites.
- ***Species Recognition:*** Drones can be used to identify plant and species types. Accuracy can be improved when combined with other platforms and sensors. They can, for example, be used to survey canopies and identify the location of native species, mother trees, and seed sources.
- ***Seed Collection and Planting:*** When fitted with robotic arms, suction tubes or rotating brushes, drones can collect seeds from remote sites, and even, with fitted with "seed bombs" can plant seeds in forest landscapes.[13]
- ***Data Mules***: As mules, drones can collect data from digital camera traps and other static, ground-based sensors, via cellular telephone networks or other technologies.[14]

[12] Paneque-Galvez et. al. 2014. Small Drones for Community-Based Forest Monitoring: An Assessment of Their Feasibility and Potential in Tropical Areas. Forests, 5, 1481-1507.

[13] Pedrini, S. et al. 2021. Smart seed for automated forest restoration. In Elliott, S., G. Gale and M. Robertson (Eds.), 2020. Automated Forest Restoration: Could Robots Revive Rain Forests? Forest Restoration Research Unit, Chiang Mai University, Thailand.

[14] See as an example the "Wadi Drone" at https://wadi.io/

4 Sensors

4.1 Understanding Sensors

As digital cameras capture visible light, sensors can detect invisible wavelengths across the electromagnetic spectrum. Active sensors send and then receive signals from the ground. Passive sensors receive naturally occurring visible, infrared, and thermal wavelengths, including reflected sunlight and heat. Both have their advantages. Unlike passive sensors, active sensors can operate in the presence of cloud cover and at night. As materials reflect and absorb at different wavelengths, which may change throughout their lifespan or in different states, passive sensors can gather information about changes to materials over time.

4.2 Optical Sensors

Optical sensors capture the emittance, reflectance and absorption of light across visible and invisible spectrums.[15] Sensors are categorized according to spectral resolution: multispectral, and hyperspectral. Multispectral systems mounted on satellites detect between four and twenty bands of light. Newer hyperspectral systems collect information across hundreds or even thousands of narrow, contiguous bands of spectral bands. As well as satellites, hyperspectral sensors can be mounted on UAVs. However, as with all sensors, hyperspectral sensors have their limitations or at least need careful interpretation. For instance, saturation in dense natural forests and band redundancy requires a careful selection of techniques to classify tree species using hyperspectral data.[16]

The information collected from optical sensors can be processed and combined in various ways to obtain sophisticated insights into the state and character of forest land. Near infra-red channels, for instance, can monitor the biodiversity of flora, exploiting the changing interaction between light and a plant's chemical properties. The changing ratio of near-infrared to visible red reflects the health status of vegetation. Photogrammetry techniques, such as Structure from Motion Multiview Stereopsis, can create 3D point clouds by overlapping images. The availability of powerful platforms enabling large-area analysis also provides the opportunity to assess forests and vegetation over time. Hamunyela et al. for example, developed an approach to detect abnormal changes in time series data, and so identify episodes of forest disturbance. The data collected provides critical insights into forest health, growth, and production.[17]

4.3 Synthetic Aperture Radar (SAR)

Synthetic Aperture Radar (SAR) is an active system that can penetrate clouds and operate at night. SAR systems send an electromagnetic signal that, depending on the length of the wavelength (X-band, C-band, L-band), penetrates vegetation to different depths.

[15] Camarretta, P. A. (2020). Monitoring forest structure to guide adaptive management of forest restoration: a review of remote sensing approaches. _New Forests_, 573–596

[16] Fassnacht, F.E.; Neumann, C.; Forster, M.; Buddenbaum, H.; Ghosh, A.; Clasen, A.; Joshi, P.K.; Koch, B. Comparison of Feature Reduction Algorithms for Classifying Tree Species with Hyperspectral Data on Three Central European Test Sites. IEEE J. Sel. Top. Appl. Earth Obs. Remote Sens. 2014, 7, 2547–2561. [CrossRef]

[17] Camarretta, P. A. (2020). Monitoring forest structure to guide adaptive management of forest restoration: a review of remote sensing approaches. _New Forests_, 573–596

Figure 4.1: SAR Signal Penetration by Sensor Wavelength[18]

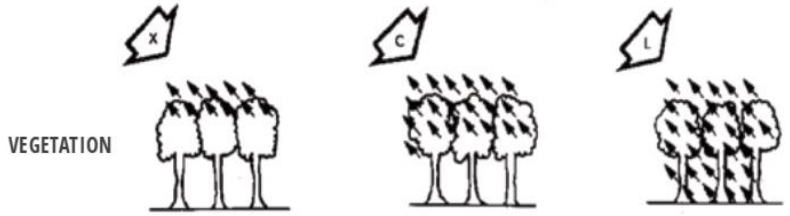

The choice of wavelength will depend on the study's purpose and the canopy's nature. C-Band SAR data, for example, will penetrate sparse boreal canopy, but not the denser, layered canopies of rainforests.[19]

SAR's ability to penetrate vegetation to different depths is particularly suited to estimating the extent of above-ground biomass, forest structures, and change over time. SAR data is often used to detect and monitor deforestation, forest degradation, and the health of mangrove forests. Like other systems, SAR complements optical remote sensing systems, both of which are presented in raster format.

Spaceborne SARs have been in use for around 40 years, although they are not typically mounted on UAVs. Nevertheless, recent missions have demonstrated its utility. The National Aeronautics and Space Administration (NASA) in collaboration with the European Space Agency and the Gabonese Space Agency used SARs mounted on UAVs to collect data to derive forest canopy height, structure and topography. The data has fed into a number of studies. Luo, H. et al., for example, utilized the SAR data to develop models to estimate forest height for wider application.

4.4 Light Detecting and Ranging (LiDAR)

LiDAR systems measure the distance from the sensor to a target based on the timing of reflected laser signals. The resulting images are represented by 3D point clouds and are used to create digital surface, terrain and height models.[20] Depending on the sensor deployed and the number of "return points," LiDAR can give extremely rich depictions of forest structures. The first returns - the initial signal - provide information on the first object detected by the laser pulse. Sensors that can detect multiple returns as the laser passes through vegetation can fully represent ground-level structures. Full waveform depicts the continuous distribution of return radiation, providing a more detailed depiction of vegetation in the study area.

LiDAR provides good approximations of tree height, tree volumes, and the delineation of tree crowns. LiDAR is often used to monitor the recovery of forest structures, monitor carbon stocks, and the recovery of carbon stocks. When combined with hyperspectral data and subjected to regression analysis and machine learning LiDAR data can significantly extend its predictive capacity. LiDAR observations combined with high-resolution optical images and machine learning have proved adept at discriminating between and identifying tree species.[21]

[18] SERVIR. (2019). _SAR Handbook: Comprehensive Methodologies for Forest Monitoring and Biomass Estimation. Alabama: SERVIR Global.
[19] SERVIR. (2019). *SAR Handbook: Comprehensive Methodologies for Forest Monitoring and Biomass Estimation.* Alabama: SERVIR Global.
[20] Frame, D. and Garzon-Lopez, C. 2021. Applications of remote sensing for tropical forest restoration: challenges and opportunities. In: Elliott, S., G. Gale and M. Robertson (Eds.), 2020. Automated Forest Restoration: Could Robots Revive Rain Forests? Forest Restoration Research Unit, Chiang Mai University, Thailand.
[21] Gyamfi-Ampadu, E. and Gebreslasie, M. 2021. Two Decades Progress on the Application of Remote Sensing for Monitoring Tropical and Sub-Tropical Natural Forests: A Review. Forests 2021, 12, 739. https://doi.org/10.3390/ f12060739

5 Ground-based Platforms

Ground-based platforms allow for detailed depictions of below canopy elements. Sensors can be placed in fixed positions or carried. Obvious downsides include a limited line of sight, and precision, particularly within dense forest canopy.

5.1 Static and Ground-based Sensors

Ground-based sensors can also provide extensive data. Commonly used sensors include:

- Terrestrial Laser Scanners (TLS);
- Mobile Laser Scanners (ZEB10);
- Near Ground photogrammetry;
- Robotic cameras;
- $C0_2$ sensors;
- Pollution sensors;
- Webcams and cyclops;
- Imaging sensors and position sensors;
- Bird cams, arrays of microphones;
- Fisheye photography from forest floor to capture canopy; and
- Tree sap flow sensor systems.

Sensors can collect an abundance of rich, but necessarily local data capturing aspects of flora and fauna, and changes to biodiversity, forest structures, and CO_2 over time. Whilst important on their own terms, ground-based sensors also serve to validate remote sensing results and train algorithms. The Phenological Eyes Network (PEN), for example, is designed to validate remote (above ground) sensing using three ground-based sensors: an automatic digital fish-eye camera, a HemiSpherical SpectroRadiometer, and a sun photometer.[22] The Forest Obesveration System is an attempt to maintain a forest biomass database, collating data from ground observation sites around the world to assist the calibration and validation of remote sensing of biomass.[23]

5.2 Data Collection

Increasingly, mobile phones provide a platform for data collection. Drones can be used as "data mules", periodically collecting data from survey sites. Researchers, including members of local communities, are also using apps on mobile phones connected to sophisticated data collection systems. Apps like Fulcrum and Kobo[24], allow teams to collect and upload observations to databases and maps. Fulcrum has been used to collect biomass data, flora, and fauna survey data, and monitor the state of infrastructure.[25]

[22] Nasahara, K.N., Nagai, S. Review: Development of an in situ observation network for terrestrial ecological remote sensing: the Phenological Eyes Network (PEN). Ecol Res 30, 211–223 (2015).
[23] See Schepaschenko, D. et al. 2019. The Forest Observation System, building a global reference dataset for remote sensing of forest biomass. *Sci Data* 6, 198 (2019).
[24] See: https://www.kobotoolbox.org/
[25] See: https://www.fulcrumapp.com/customer-stories/preventing-deforestation-and-protecting-natural-resources

6 Sensors in Combination

Platforms and the sensors they carry often operate best in combination. In a sense, the system becomes the sensor.[26] When combined, sensors can compensate for weaknesses in some technologies and complement others. At a more straightforward level, correlations between variables can provide insights into observed behaviours and trends. For example, periods of low temperatures might be correlated with reduced bird reproduction. Maps developed from satellites or UAVs can be combined with bird cams or other sensors to estimate population densities.

Complementary technologies can also provide greater insight into specific objects of study. Optical and 3D point clouds can help with species identification - shrubs or trees may share the same spectral signature but have different architectural properties. Similarly, 3D systems may be able to estimate the volume of deadwood at a site, but optical systems may be necessary to detect deadwood in the first place.

The rapid development of sensing and processing technologies also means that new uses continue to be developed. In a recent example, Alves de Almeida, D. et al.[27] sought to establish the diversity and structure of restoration plantings by exploring the congruence and complementarity of lidar and hyperspectral data. They found that the "fusion" of UAV-borne hyperspectral and lidar data enabled the co-monitoring of forest structural attributes and tree diversity.

Csillik et al.[28] illustrate the contributions to forest monitoring of incremental advances and cost reductions of key technologies. Noting previous studies that combined satellite images with airborne LiDAR to map above-ground carbon density (ACD) in areas that lacked LiDAR measurements they took advantage of newly available high-resolution images from Dove satellites, Random Forest algorithms, and LiDAR measurements to map ACDs for tropical forests over extended spatial scales. The resulting indicators, in principle replicable at low cost, have the potential to improve the monitoring of carbon stocks over time.

Data is typically collected in raster form – as a grid - or as 3D point clouds. Collected data can be classified as either categorical or continuous.[29] Classification algorithms are applied to categorical data, and increasingly AI and machine learning are used to categorize landscapes. Continuous data is often used to find correlations between field measurements and vegetation or other indices (see below). High-resolution data pixels can be interpreted as spatial units, such as trees, and then classified using "object-based image analysis".

Many if not all datasets produced by satellites are also now made freely available. These include the Landsat series and data provided by the European Space Agency suite of satellites, and Google earth Engine also allows access to extensive global datasets. Table 6.1 provides an extensive list of open access ecology data sets.

[26] Gabrys, J. 2016. Sensing an Experimental Forest: Processing Environments and Distributing Relations. In Program Earth: Environmental Sensing Technology and the Making of a Computational Planet (pp. 29–55). University of Minnesota Press.
[27] Alves de Almeida, D. et al. 2021 Monitoring restored tropical forest diversity and structure through UAV-borne hyperspectral and lidar fusion, Remote Sensing of the Environment Vol. 264
[28] Csillik, O., Kumar, P., Mascaro, J. _et al._ 2019. Monitoring tropical forest carbon stocks and emissions using Planet satellite data. _Sci Rep_ **9**, 17831. https://doi.org/10.1038/s41598-019-54386-6
[29] Lechner, M. et al. 2020. Applications in Remote Sensing to Forest Ecology and Management. One Earth. Accessed here: https://core.ac.uk/reader/328760320

Table 6.1: Open Access Forest Ecology Data Derived from Remote Sensing

Name	Resolution	Time scale	Time availability	Spatial Availability	Satellite data input	Classification system	Producer	Accuracy	Acquisition
Dynamic World land cover	10 m	Near real-time, daily	2014 - now	Global	Sentinel-2	9 classes	Google - WRI	73.8%	Open access
ESA-WorldCover land cover	10 m	yearly	2020, 2021	Global	Sentinel-1 and Sentinel-2	11 classes	ESA	75-77%	Open access
ESRI Land Cover	10 m	yearly	2017 - 2021	Global	Sentinel-2	9 classes	ESRI	73-74%	Open access
Servir Mekong land cover	30 m	yearly	1987 - 2018	Mekong countries	Landsat, MODIS	17 classes	SERVIR MEKONG	78%	Open access
Global Forest Change (Hansen)	30 m	yearly	2000 - 2019	Global	Landsat	Forest cover 2000, Forest gain 2000-2012, Lossyear 2000-2019	UMD	90%	Open access
CCI Biomass	100 m	yearly	2010, 2017, 2018	Global	Sentinel1 ALOS-1 ALOS-2 EnviSat ASAR	-	ESA	Bias in the high biomass areas	Open access
Above-ground Live Woody Biomass Density (GFW)	30 m	yearly	2000	Global	Landsat LIDAR		WRI		Open access
Soilgrids250	250 m	-	-	Global			ISRIC (2020)		Open access
MCD64A1 (L3 Monthly 500m	500 m	monthly	-	Global	MODIS	Burn date	NASA	-	Open access

Name	Resolution	Time scale	Time availability	Spatial Availability	Satellite data input	Classification system	Producer	Accuracy	Acquisition
"Direct Broadcast" Burned Area)									
Global Mangrove Watch	25 m	yearly	1996 - 2020	Global	ALOS-1		JAXA		Open access
Primary Forests	30 m	Yearly	2001	Tropical	Landsat		UMD		Open access
Intact forest	vector	yearly	2000, 2013, 2016, 2020	Global	-		UMD		Open access
Planted trees	vector	yearly	Around 2015	82 countries		Many classes	WRI		Open access
Global peatland extent	30 m	Yearly	2016-2021 (depends on countries)	Global	Landsat		various		Open access
Tree cover height	30 m	yearly	2000, 2020	global	Landsat		UMD		Open access

The advent of cloud computing provides access to repositories of images, web-based mapping, high-performance computing, and access to software. Services such as GEE help simplify intensive processes that once required extensive human input and computing power. Key techniques include multi-temporal mosaics, which produce composite images in which pixels represent median values over a specified time period.[30] Temporal trend analysis using software such as LandTrendr can help identify and analyze landscapes' disturbance and recovery over time.[31]

Machine Learning can help to classify land cover types and species types. Random Forest or Support Vector Machines, and unsupervised learning algorithms such as K-means, K-NN, are widely used in remote sensing image classification. Figure 6.1 demonstrates the process by which a digital number representing bands of light is converted into a spatial expression of land use categories using machine learning.

Figure 6.1: Remote Sensing Imagery Classification[32]

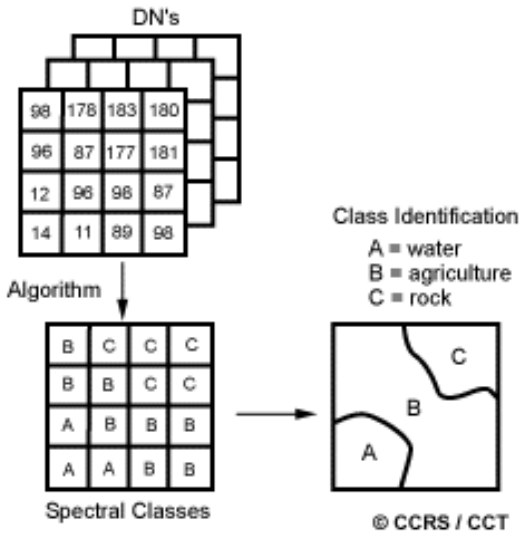

Vegetation reflects different wavelengths depending on its health and state. Spectral reflectance, interpreting the contrast between near-infrared and visible infrared light, is used to derive vegetation indices, that can provide an indicator of photosynthetically active biomass, and vegetation health. It can, however, be challenging to distinguish between crops and trees as both have high Normal Different Vegetation Index (NDVI) values.[33] If mean values are taken over three-month periods, however, high NDVI values can accurately be assumed to be forest, and indices provide a useful way to monitor change to forests over time. The Enhanced Vegetation Index (EVI) offers greater accuracy in areas with dense canopy.

Other common uses include:

- ***The identification of deadwood****:* 3D maps have been shown better to capture information at finer resolutions than on-ground measurements.
- ***Canopy Structures****:* Data collected by LiDAR has been successfully used to classify canopies into multiple strata, quantify canopy surface dynamics and extract single tree crowns. To date, however, the techniques have not been applied to landscape and regional spatial levels.
- ***Monitor vegetation cover****:* Analysis of vegetation indices can monitor land use change and identify regions or corridors to target restoration efforts. Combinations of techniques can provide information on density, stand development, and the 3D distribution of vegetation.
- ***Identify tree species****:* Hyperspectral imagery can identify tree species with training and validation of machine-learning algorithms. However, there remain challenges in expanding the total number of species detected, identifying understory vegetation, and scaling up fine-resolution images to identify species over larger areas.
- ***Structural complexity****:* Given the technical challenges in determining structural complexity over large areas, a common approach is identifying and tracking permanent plots of land scattered

[30] Lechner, M. et al. 2020. Applications in Remote Sensing to Forest Ecology and Management. One Earth. Accessed here: https://core.ac.uk/reader/328760320
[31] Kennedy, R.E., Yang, Z. and Cohen, W.B., 2010. Detecting trends in forest disturbance and recovery using yearly Landsat time series: 1. LandTrendr - Temporal segmentation algorithms. Remote Sensing of Environment, 114(12), pp.2897-2910.
[32] Source: NRCAN. (2022). Image Classification and Analysis. Retrieved from Natural Resources Canada: https://www.nrcan.gc.ca/maps-tools-and-publications/satellite-imagery-and-air-photos/tutorial-fundamentals-remote-sensing/image-interpretation-analysis/image-classification-and-analysis/9361
[33] Vegetation Index: https://eos.com/blog/ndvi-faq-all-you-need-to-know-about-ndvi/.

through landscapes with combinations of ground-, air- and spaceborne technology. Such a monitoring network of plots can help to track changes to structures over time and ecosystem systems and services to the extent that structural complexity serves as a proxy.

Various online tutorials provide step-by-step instructions to help analysts take advantage of rapidly emerging opportunities. A far-from-exhaustive list includes:

- ***Open MRV: Training data collection*** using GEE provides a step-by-step guide to collecting categorical training data.[34]
- ***Open MRV Land Cover and Land Use Classification in Google Earth Engine***[35] provides a guide to producing a training data set, training an algorithm to categorize data and create a "classifier" applying the classifier to an image. Open MRV requires access to and knowledge of Google Earth Engine.
- ***ARSET - Using Google Earth Engine for Land Monitoring Applications*** provides training on using GEE capabilities.[36]
- ***UNSPIDER - Step-by-Step: Land Cover Change Detection through Supervised Classification*** explains how to undertake a supervised land cover classification and change detection analysis.[37]

[34] OpenMRV. (2023). Training Data Collection Using Google Earth Engine. Retrieved from Open-source resources for Forest Measurement, Reporting and Verification (MRV): https://openmrv.org/web/guest/w/modules/mrv/modules_1/training-data-collection-using-google-earth-engine

[35] OpenMRV. (2023). Land Cover and Land Use Classification in Google Earth Engine. Retrieved from Open-source resources for Forest Measurement, Reporting and Verification (MRV): https://openmrv.org/web/guest/w/modules/mrv/modules_1/land-cover-and-land-use-classification-in-google-earth-engine

[36] See https://appliedsciences.nasa.gov/join-mission/training/english/arset-using-google-earth-engine-land-monitoring-applications

[37] See https://www.un-spider.org/advisory-support/recommended-practices/recommended-practice-land-cover-change/step-by-step

7 Case Study 1: Land Cover Monitoring of the Sangker River Basin, Cambodia[38]

Assessing forest land cover changes over time provides essential insights into forest recovery, and is a critical element in REDD+. This case study identifies the steps to assess land cover change in the Sangker River Basin in Cambodia (Figure 7.1) between 2017 and 2021. The results have informed a hydrological survey of the Sangker River Basin, and will form a baseline to monitor the progress of restoration efforts over time.[39]

Figure 7.1: Position of the Sangker River Basin

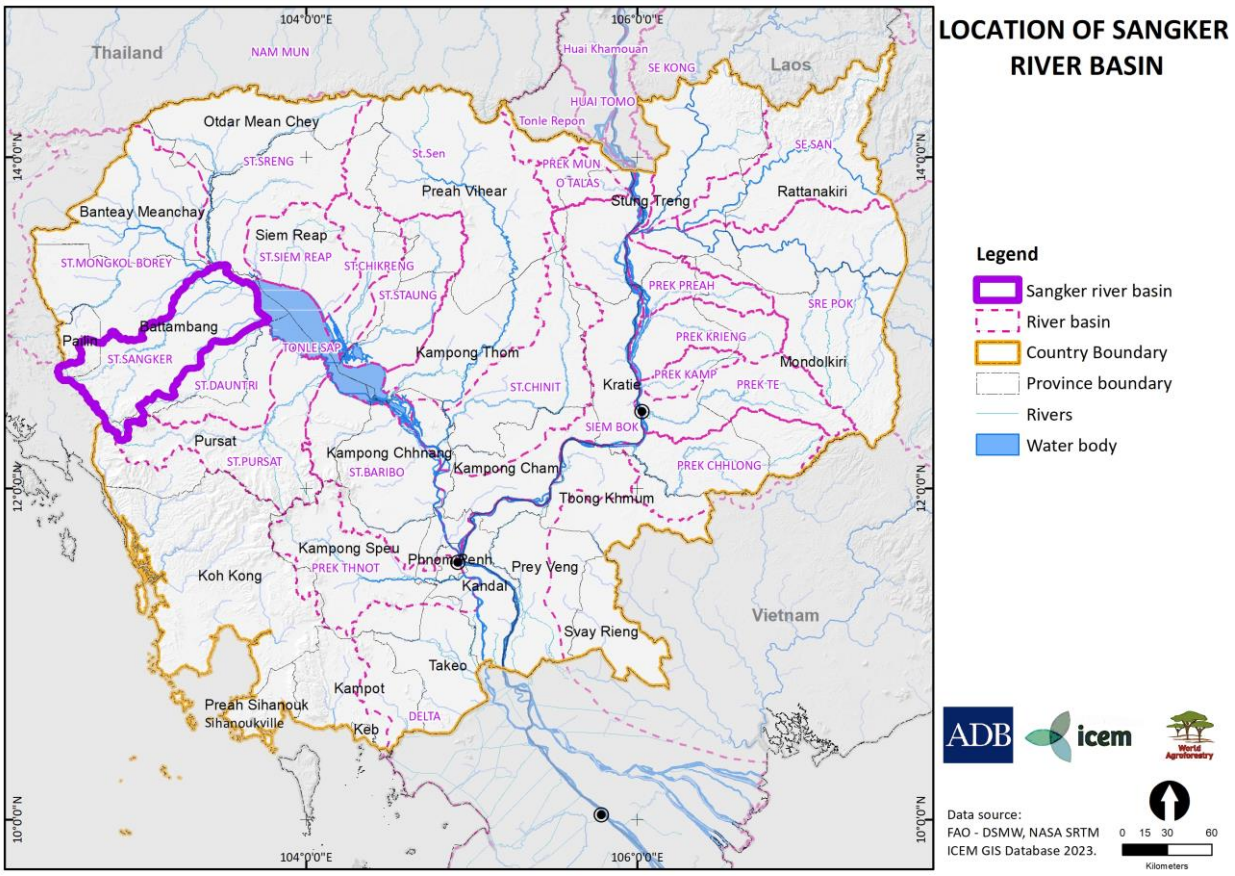

7.1 Developing Reference Maps for Comparison Years

The choice of satellite imagery largely depends on the period and area studied. Sentinel-2 is increasingly used for the analysis of large spatial areas. However, if data is required for more extended periods Landsat is commonly used. Given that the study years were relatively recent, this study used Sentinel-2 data.

The ICEM team prepared composite images for 2017 and 2021 to be used for the comparison. Images of the Sangker basin were accessed using the Google Earth Engine (GEE). The composite images were prepared by calculating median values for all matching bands for all available images in each year. Cloud masking was conducted using information integrated in the Sentinel 2 data. The final composite image for 2021 can be seen in Figure 7.2.

[38] The code used in both case studies is provided in Annex A, and can be adapted to similar landscapes.
[39] Please contact ICEM for further details on restoration plans the hydrological survey of the Sangker River Basin.

Figure 7.2: Yearly Composite Sentinel-2 Image in the Sanker Basin

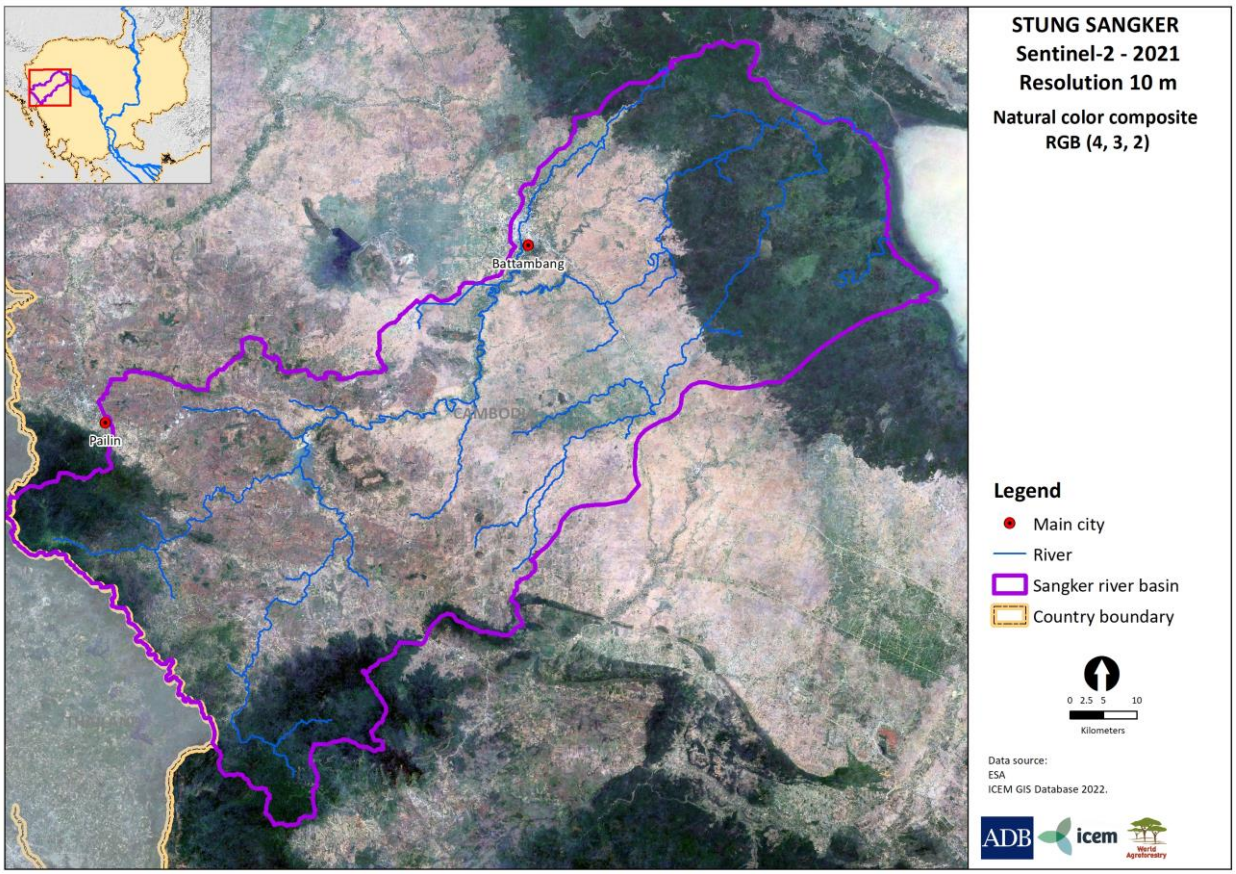

7.2 Identifying and Classifying Land Cover Types

To classify land cover types, it is necessary to collect "reference data," in which units of land are attributed a land cover category. Reference data can be collected using remote sensing imagery or by field survey. The Sangker River Basin study applied an algorithm sourced from Random Forest to the 2021 composite image of the river basin. The Random Forest algorithm is widely used for land cover classification.[40]

Each pixel contained digital values representing spectral bands used to determine the land cover type. Five hundred and four data points were identified and organized into six categories: water (50 points), forest (62 points), grass (50 points), shrub and scrub (68 points), built (80 points), and crops (194 points). Eighty percent of the data points were used to train the algorithm and the remaining 20 percent for validation (Figure 7.3).

[40] Vegetation Index: https://eos.com/blog/ndvi-faq-all-you-need-to-know-about-ndvi/.

Figure 7.3: Reference Data for Land Cover Classification

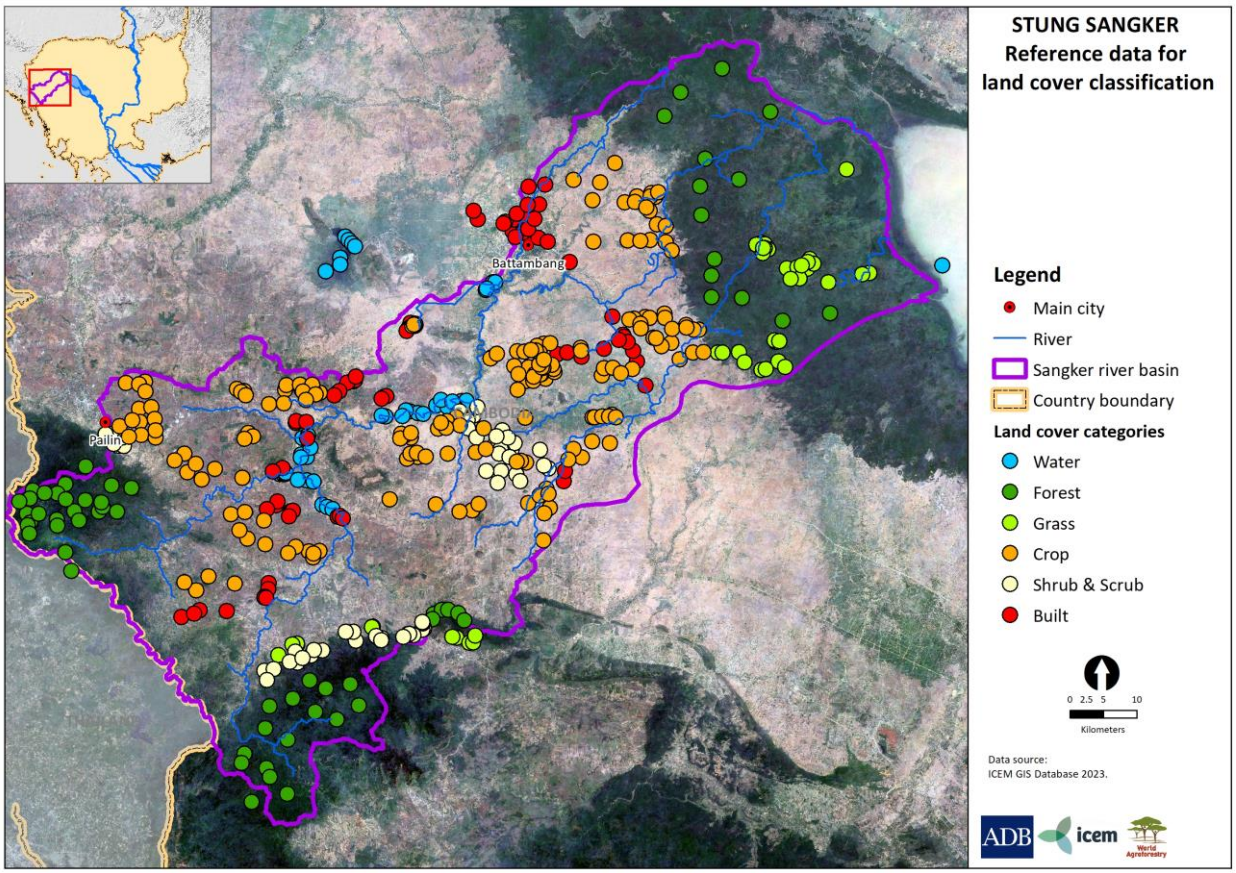

An error matrix was then generated to assess the accuracy of the map. Table 7.1 compares the predicted data points with the actual data points for the validation data set. The level of accuracy - in this case 0.77 - is the ratio of the sum of the diagonal to the total number of validation data.

Table 7.1: Error Matrix of Land Cover Map, 2021 Sangker River Basin

		Predicted						
		Forest	Grass	Crop	Shrub & scrub	Built	Water	Total
Actual	Forest	13	0	0	0	0	0	13
	Grass	0	11	2	0	0	0	13
	Crop	0	2	44	2	2	0	50
	Shrub & scrub	2	1	7	3	0	0	13
	Built	0	0	4	2	5	0	11
	Water	1	0	1	0	0	11	13
	Total	**16**	**14**	**58**	**7**	**7**	**11**	**113**

7.3 Analysis of Land Cover Change Between 2017 and 2021

Using the identified land cover labels, maps were produced for both 2017 and 2021 (Figure 7.4).

Figure 7.4: Land Cover Map of Sangker Basin 2017 – 2021

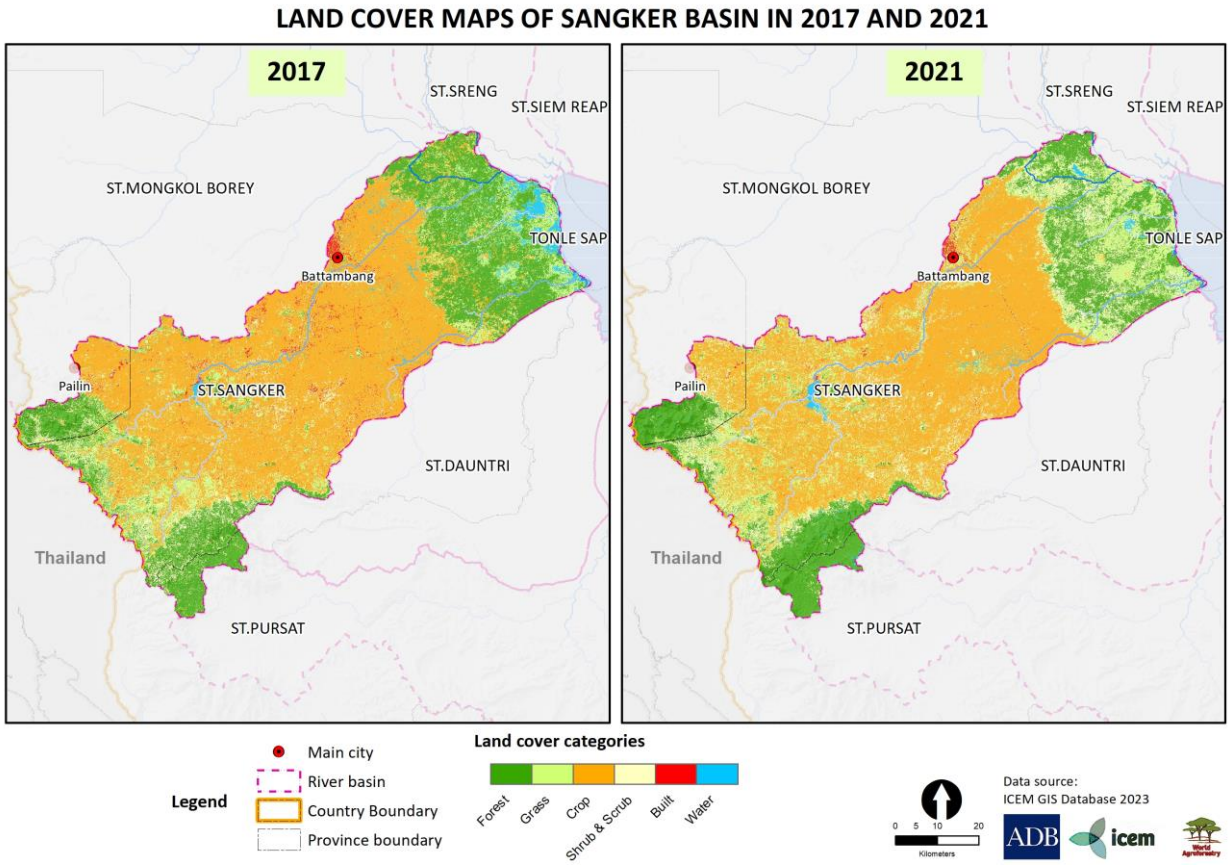

To determine changes in land cover the commonly used UN-SPIDER methodology was applied. UN-SPIDER provides a step-by-step process to conduct a supervised land cover classification, making use of open-source software QGIS and the Semi-Automatic Classification Plugin.[41] Table 7.2 presents the resulting land cover changes. The rows present land-cover types in 2017, and the columns land-cover types in 2021. For example, in 2017, 142,590 of the Sangker River Basin was classified as forest. By 2021 this had reduced to 129,120. The table shows 93,640 hectares were classified as forest in both years. Between 2017 and 2021, 15,720 hectares of forest was converted to grass, 2,430 hectares to crop cultivation, and so on.

Table 7.2: Land Cover Change Matrix

	2021 (ha)							
2017 (ha)	**Forest**	**Grass**	**Crop**	**Shrub & Scrub**	**Built**	**Water**	**Total**	**% Total Land Area 2017**
Forest	93,640	15,720	2,430	29,280	-	1,520	142,590	23.5%
Grass	15,480	32,240	17,470	13,840	50	1,270	80,360	13.3%
Crop	6,520	27,970	248,860	30,890	1,630	1,850	317,720	52.5%
Shrub & Scrub	11,930	4,890	13,700	7,760	160	70	38,510	6.4%
Built	10	340	6,520	1,510	1,610	50	10,040	1.7%
Water	1,540	7,260	3,010	2,090	30	2,370	16,290	2.7%

[41] Data base for remote sensing indices

	2021 (ha)							
2017 (ha)	**Forest**	**Grass**	**Crop**	**Shrub & Scrub**	**Built**	**Water**	**Total**	**% Total Land Area 2017**
Total	129,120	88,420	291,980	85,370	3,490	7,130	605,510	100.0%
% Total Land Area 2021	21.3%	14.6%	48.2%	14.1%	0.6%	1.2%		
% Change 2017 -2021	-2.2%	1.3%	-4.3%	7.7%	-1.1%	-0.5%		

Table 7.2 shows that between 2017 and 2021, over 2.2% of the total forest area was converted to other uses, mostly shrub and scrub and grass land. Perhaps surprisingly, the built environment and the proportion of land devoted to crops fell over the four years. A net 47 thousand hectares was converted to scrub land in the same period. However, this figure disguises some of the dynamics of land use change. Whilst, 248,860 hectares of cropland remained unchanged (78%), 7,760 hectares (20% of 2017 land use) of land was scrub in both years, pointing to the dynamic land use changes in the intervening period.

8 Case Study 2: Above-ground Biomass Monitoring in the Sangker River Basin, Cambodia

Estimates of above ground biomass (AGB) are useful indicators of a landscape's ability to store carbon, and so inform REDD+ programs and monitor progress of restoration efforts over time. Often, data is limited in resolution, available time periods and spatial coverage. Moreover, biomass surveys of target sites and landscapes are time consuming and expensive.

An alternative is to identify the relationship between more readily available data and field estimates of biomass in comparable sites. This case study presents a process adopted from a recent study, which combined PALSAR data and field data to develop biomass maps in Cambodia.[42]

The study undertook a field survey of 79 sampling plots in Cambodia. The sites were chosen to minimize any topographic effects on SAR data.

PALSAR data was then retrieved for the same sites. At each the biomass beneath the forest canopy had been captured using the L-Band of PALSAR-2. The digital values of the ScanSAR data were converted to gamma naught (γ0), the backscatter coefficient that represents the detectability of objects by radar signals. Gamma naught expressed in decibel units (dB) is calculated using the following equation:[43]

$$\gamma 0 = 10*\log10(DN2) - 83.0 \text{ (dB)}$$

In which: γ0 is the backscatter coefficient gamma naught, DN is the digital number value of each pixel

The resulting coefficient was used to determine the AGB of the Sangker River Basin using SAR data retrieved from GEE, using the following equation:[44]

$$\_y\_ = 1.8122\ln(\_x\_) – 21.202$$

In which: y_ is gamma naught values of HV polarization, _x_ is the in situ data of AGB biomass.

Using this process, the AGB of Sangker basin was estimated for the years 2017 and 2021. The change between the two years was then estimated by raster calculation and is expressed spatially in Figure 8.1.

[42] Ram Avtar, S. M. (2018). Integrating ALOS-PALSAR and ground based observations for forest biomass estimation for REDD+ in Cambodia. Kobe: APN.
[43] Ibid
[44] Ibid

Figure 8.1: The Change in Above-Ground Biomass in Sanker Basin in 2017-2021

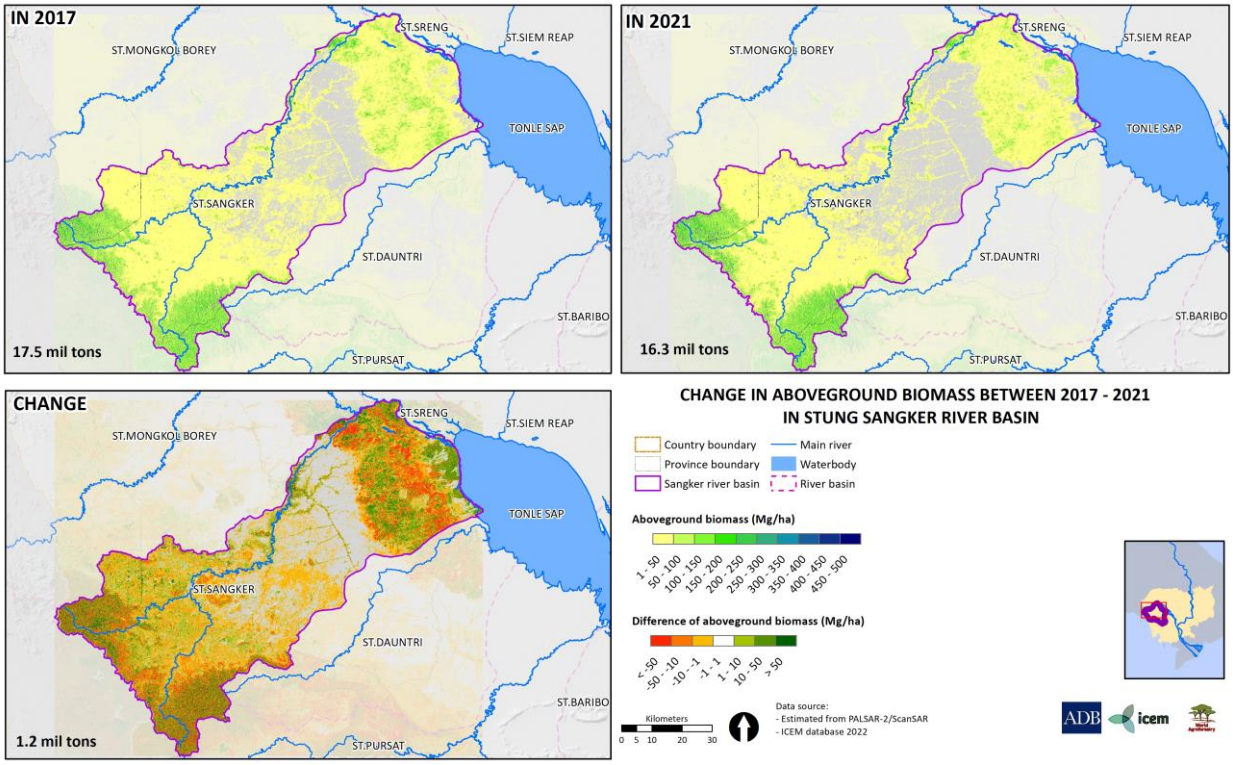

The analysis demonstrates that the total biomass in the river basin has fallen over the course of four years, from 17.5 million to 16.3 million tons. However, the change has not been uniformed. Most of the river basin has seen an increase in biomass, with the greatest increase in the headwaters. The reason for that increase would need to be determined through field survey, because anecdotal evidence suggests that the headwaters has experienced significant forest loss. An increase in biomass improves the river basin's carbon storage capacity. The analysis also indicates that there has been significant loss of biomass in the lower reaches of the river basin, potentially the result of agricultural activity. Such analysis can help to keep track of the progress of interventions, and identify areas where there has been a significant change in land use. It can also help to guide adaptation strategies, suggesting areas to prioritize for further study or further interventions.

9 Summary

- Forest restoration is increasingly a high-technology, data-intensive process. Satellites, drones, and ground-based sensors are producing ever more sophisticated images and data sets, providing invaluable insights into the health and nature of forests.
- There is no one optimal technology or combination of technologies. The chosen approach needs to consider trade-offs between temporal and spatial resolution or cost and coverage, and must be tailored to the purpose at hand.
- Increasingly the choice of technology must consider the software, computing power, and expertise available to interpret results.
- Satellite imagery confers a range of benefits and will suffice for most uses. New generations of satellites carry increasingly sensitive sensors, opening up possibilities for forest monitoring.
- Airborne technologies, particularly drones, are becoming more sophisticated and affordable and serve several uses, including site surveys, site monitoring, species recognition, and even seed collection and planting, and as "mules" to collect data transmitted by ground sensors at remote locations.
- Ultimately, the most useful technology is the sensor. Sensors are characterized by their spectral resolution - multispectral or hyperspectral - and whether they are "passive", and so receive signals naturally transmitted from the earth, or "active" and able to fire and detect signals on their return.
- Either on their own or combined with other sources of information, the data collected can provide crucial information on critical aspects of flora and fauna in a target area. Information includes the identification and health of species, the presence, and volume of deadwood, the extent of biodiversity, canopy and the structure of the forest itself.
- Time series data can show the progress of restoration efforts and provide insights into the causes of forest change.
- The advent of cloud computing provides access to repositories of images, web-based mapping, high-performance computing, and access to software. Data collected by UAVs can be used to train algorithms to examine satellite images covering more expansive areas than possible with UAVs alone.

Annex A: Script to generate maps provided in Sections 7 and 9, using Google Earth Engine.

Google Earth Engine (GEE) is a powerful tool for use in forest restoration activities. The following code accompanies the two case studies discussed in Sections 7 and 8. An account with Google Earth Engine is required, and a level of familiarity with GEE is assumed. The code can be pasted into a code editor in Earth Engine Code Editor. The code in Annex A.1 generates figures 7.4 and can be adapted to produce land cover maps of target landscapes. The code in Annex A.2 generates figure 8.4, and can be adapted to generate maps that illustrate changes in biomass over time in target locations.

Annex A.1: Code to generate land cover maps (Figure 7.4)

The following code generates the map depicted in Figure 7.4.

```
1.
    ////******Part 1: Scoping imagery, preprocessing ******
2.  ////////////////////////////////////////////////////////
3.
4.  function maskS2clouds(image) {
5.    var qa = image.select('QA60');
6.
7.    // Bits 10 and 11 are clouds and cirrus, respectively.
8.    var cloudBitMask = 1 << 10;
9.    var cirrusBitMask = 1 << 11;
10.   // Screen out bright value, which is also cloud
11.   var blue=image.select('B2')
12.   var green=image.select('B3')
13.   var red=image.select('B4')
14.
15.   // Cloud masking
16.   var mask = qa.bitwiseAnd(cloudBitMask).eq(0)
17.       .and(qa.bitwiseAnd(cirrusBitMask).eq(0))
18.       .and(blue.gt(2000).eq(0))
19.       .and(green.gt(2000).eq(0))
20.       .and(red.gt(2000).eq(0));
21.       // .and(BGratio.gt(1.3).eq(0)); // if conduct cloud shadow removal
22.   return image.updateMask(mask);
23. }
24.
25. // Data scoping
26. var S2MSI_sangker_2021_L1C_yearlycomp = ee.ImageCollection('COPERNICUS/S2')
27.                   .filterDate('2021-01-01', '2021-12-31')
28.                   .map(maskS2clouds)
29.                   .select(['B1','B2','B3','B4','B5','B6','B7','B8','B8A','B9','B10
    ','B11','B12'], ['Coastal aerosol','BLUE','GREEN','RED','Veg Red Edge B5', 'Veg
    Red Edge B6', 'Veg Red Edge B7','NIR','Narrow NIR','Water Vapour','SWIR
    cirrus','SWIR1','SWIR2'])
30.                   .median()
31.                   .toUint16();
32.
33. var rgbVis = {
34.   min: 0,
35.   max: 3000,
36.   bands: ['RED', 'GREEN', 'BLUE'],
37. };
38.
```

```
Map.addLayer(S2MSI_sangker_2021_L1C_yearlycomp, rgbVis, 'Sentinel2-RGB');

// Boundary of sanker
var shp = ee.FeatureCollection(polygon)
var shpVis = shp.style({
  color: '17202A ',
  width: 2,
  fillColor: 'ff475700',  // with alpha set for partial transparency
  lineType: 'dotted',
  pointSize: 10,
  pointShape: 'circle'
});

////******Part 2: Add Developed Land Cover Data For making reference data******
//////////////////////////////////////////////////////////////////////////////

// var startDate = '2021-01-01';
// var endDate = '2022-01-01';
// var geometry = ee.Geometry.Rectangle([102.4,12.2,103.9,13.4]);
// var dw = ee.ImageCollection('GOOGLE/DYNAMICWORLD/V1')
//             .filterDate(startDate, endDate)
//             .filterBounds(geometry);
// var classification = dw.select('label');
// var dwComposite = classification.reduce(ee.Reducer.mode());
// var dwVisParams = {
//   min: 0,
//   max: 8,
//   palette: [
//     '#419BDF', '#397D49', '#88B053', '#7A87C6', '#E49635', '#DFC35A',
//     '#C4281B', '#A59B8F', '#B39FE1'
//   ]
// };

// // Clip the composite and add it to the Map.
// Map.addLayer(dwComposite.clip(geometry), dwVisParams, 'Classified Composite');

////******Part 3: Prepare for the classification******
//////////////////////////////////////////////////////

//merge reference data
var reference = water.merge(forest)
                     .merge(grass)
                     // .merge(flooded_vegetation)
                     .merge(shrub_scrub)
                     .merge(built)
                     .merge(crop);


// get the labels from these training points.
var bands_to_use = ['BLUE','GREEN','RED','NIR','SWIR1','SWIR2']

// Now do a spatial overlay of the points on the image, and extract
var landcover_labels = 'label'
var reference_extract =
    S2MSI_sangker_2021_L1C_yearlycomp.select(bands_to_use).sampleRegions({
  collection: reference,
  properties: [landcover_labels],
  scale: 10
}).randomColumn();
```

```
97.
98. //Randomly split the samples to set some aside for testing the models accuracy
99. //using the "random" column. Roughly 80% for training, 20% for testing.
100.   var split = 0.8;
101.   var training = reference_extract.filter(ee.Filter.lt('random', split));
102.   var testing = reference_extract.filter(ee.Filter.gte('random', split));
103.
104.   //Print these variables to see how much training and testing data you are using
105.   print('Samples n =', reference_extract.aggregate_count('.all'));
106.   print('Training n =', training.aggregate_count('.all'));
107.   print('Testing n =', testing.aggregate_count('.all'));
108.
109.   var classifier = ee.Classifier.smileRandomForest(300,5)
110.     .train(training, landcover_labels, bands_to_use);
111.
112.
113.   //Test the accuracy of the model
114.   ////////////////////////////////////////
115.
116.   //Print Confusion Matrix and Overall Accuracy
117.   var confusionMatrix = classifier
118.   print('Confusion matrix: ', confusionMatrix);
119.   print('Training Overall Accuracy: ', confusionMatrix.accuracy());
120.   var kappa = confusionMatrix.kappa();
121.   print('Training Kappa', kappa);
122.
123.   var validation = testing.classify(classifier);
124.   var testAccuracy = validation.errorMatrix('label', 'classification');
125.   print('Validation Error Matrix RF: ', testAccuracy);
126.   print('Validation Overall Accuracy RF: ', testAccuracy.accuracy());
127.   var kappa1 = testAccuracy.kappa();
128.   print('Validation Kappa', kappa1);
129.
130.   var classified =
      S2MSI_sangker_2021_L1C_yearlycomp.clip(shp).select(bands_to_use).classify(classifi
      er);
131.
132.   ////******Part 5:Create a legend******
133.   ////////////////////////////////////////
134.
135.   // Set position of panel
136.   var legend = ui.Panel({
137.     style: {
138.       position: 'bottom-left',
139.       padding: '8px 15px'
140.     }
141.   });
142.
143.   //Create legend title
144.   var legendTitle = ui.Label({
145.     value: 'Classification Legend',
146.     style: {
147.       fontWeight: 'bold',
148.       fontSize: '18px',
149.       margin: '0 0 4px 0',
150.       padding: '0'
151.       }
152.   });
153.
154.   //Add the title to the panel
```

```
legend.add(legendTitle);

// Create and style 1 row of the legend.
var makeRow = function(color, name) {

      var colorBox = ui.Label({
        style: {
          backgroundColor: '#' + color,
          padding: '8px',
          margin: '0 0 4px 0'
        }
      });

      var description = ui.Label({
        value: name,
        style: {margin: '0 0 4px 6px'}
      });

      return ui.Panel({
        widgets: [colorBox, description],
        layout: ui.Panel.Layout.Flow('horizontal')
      });
};

//Identify palette with the legend colors
var palette =['419BDF', '397D49', '88B053', 'E49635', 'DFC35A','C4281B'];

//Identify names within the legend
var names = ['Water','Forest','Grass',
             'Crop','Shrub_Scrub','Built'];

//Add color and names
for (var i = 0; i < 6; i++) {
  legend.add(makeRow(palette[i], names[i]));
  }

//Add legend to map
Map.add(legend);

////******Part 6: Display and Export ******
//////////////////////////////////////////

//Create palette for the final land cover map classifications
var Palette =
'<RasterSymbolizer>' +
' <ColorMap  type="intervals">' +
    '<ColorMapEntry color="#419BDF" quantity="7" label="Water"/>' +
    '<ColorMapEntry color="#397D49" quantity="1" label="Forest"/>' +
    '<ColorMapEntry color="#88B053" quantity="2" label="Grass"/>' +
    '<ColorMapEntry color="#E49635" quantity="4" label="Crop"/>' +
    '<ColorMapEntry color="#DFC35A" quantity="5" label="Shrub_Scrub"/>' +
    '<ColorMapEntry color="#C4281B" quantity="6" label="Built"/>' +
  '</ColorMap>' +
'</RasterSymbolizer>';

//Add final map to the display
Map.addLayer(classified.sldStyle(Palette), {}, "Land Classification");
Map.addLayer(shpVis, {}, 'Sanker boundary');
Map.setCenter(103, 13,9);
```

Annex A.1 Code to estimate Aboveground Biomass using Google Earth Engine

The following code generates the map depicted in Figure 8.4.

```
// var shp = ee.FeatureCollection(polygon);
var region_sangker = ee.Geometry.Rectangle([102.4,12.2,103.9,13.4]);
var sarHV = ee.ImageCollection('JAXA/ALOS/PALSAR-2/Level2_2/ScanSAR')
                    .filterDate('2020-01-01', '2020-12-30')
                    .select('HV')
                    .filterBounds(polygon)
                    .median();
// var sarHV = dataset.select('HV');

var gammaHV=sarHV.pow(ee.Number(2)).log10().multiply(10).subtract(83)

// calculate biomass based on study of Ram Avtar (2018)
var biomass=((gammaHV.add(21.202)).divide(1.8122)).exp()
print(biomass)
// var sarHVVis = {
//   min: -30,
//   max: 0,
// };

var biomassVis =
'<RasterSymbolizer>'+
  '<ColorMap type="intervals" extended="false">'+
    '<ColorMapEntry label="<= 0" quantity="1" color="#f8f8f8"/>'+
    '<ColorMapEntry label="0 - 50" quantity="50" color="#ffffcc"/>'+
    '<ColorMapEntry label="50 - 100" quantity="100" color="#e4f4b6"/>'+
    '<ColorMapEntry label="100 - 150" quantity="150" color="#c9e99f"/>'+
    '<ColorMapEntry label="150 - 200" quantity="200" color="#a9dc8e"/>'+
    '<ColorMapEntry label="200 - 250" quantity="250" color="#88cd80"/>'+
    '<ColorMapEntry label="250 - 300" quantity="300" color="#68be71"/>'+
    '<ColorMapEntry label="300 - 350" quantity="350" color="#48af60"/>'+
    '<ColorMapEntry label="350 - 400" quantity="400" color="#2b9d51"/>'+
    '<ColorMapEntry label="400 - 450" quantity="450" color="#158244"/>'+
   '<ColorMapEntry label="> 450" quantity="500" color="#006837"/>'+
 '</ColorMap>'+
'</RasterSymbolizer>';


// print(sarHV)
Map.setCenter(103, 13,9);
// Map.addLayer(gammaHV.clip(polygon), sarHVVis, 'SAR HV');
// Map.addLayer(biomass.clip(polygon), biomassVis, 'biomass');
Map.addLayer(biomass.clip(polygon).sldStyle(biomassVis),{}, 'biomass');
var shpVis = polygon.style({
  color: 'ea2119 ',
  width: 2,
  fillColor: 'ff475700',  // with alpha set for partial transparency
  lineType: 'dotted',
  pointSize: 10,
  pointShape: 'circle'
});
Map.addLayer(shpVis, {}, 'Sanker boundary');

// set position of panel
var legend = ui.Panel({
  style: {
    position: 'bottom-left',
```

```
    padding: '8px 15px'
  }
});

//Create legend title
var legendTitle = ui.Label({
  value: 'Biomass estimated (Mg/ha)',
  style: {
    fontWeight: 'bold',
    fontSize: '18px',
    margin: '0 0 4px 0',
    padding: '0'
    }
});

//Add the title to the panel
legend.add(legendTitle);

// Creates and styles 1 row of the legend.
var makeRow = function(color, name) {

      // Create the label that is actually the colored box.
      var colorBox = ui.Label({
        style: {
          backgroundColor: '#' + color,
          // Use padding to give the box height and width.
          padding: '8px',
          margin: '0 0 4px 0'
        }
      });

      // Create the label filled with the description text.
      var description = ui.Label({
        value: name,
        style: {margin: '0 0 4px 6px'}
      });

      // return the panel
      return ui.Panel({
        widgets: [colorBox, description],
        layout: ui.Panel.Layout.Flow('horizontal')
      });
};


  //  Palette with the colors
  var palette =['f8f8f8', 'ffffcc',
'e4f4b6','c9e99f','a9dc8e','88cd80','68be71','48af60','2b9d51','158244','006837'];

  // name of the legend
  var names = ['0','1 - 50','50 - 100','100 - 150','150 - 200','200 - 250','250 -
300','300 - 350','350 - 400','400 - 450','> 450'];

  // Add color and and names
  for (var i = 0; i < 11; i++) {
    legend.add(makeRow(palette[i], names[i]));
    }
  // add legend to map (alternatively you can also print the legend to the
console)
  Map.add(legend);
```

Anakut Koma Samaki, Cambodia (photo by ICEM)

Correspondence
26/86, To Ngoc Van Street,
Tay Ho District, Hanoi, Vietnam
(t) +84 24 3823 9127
(f) +84 24 3719 0367
info@icem.com.au
www.icem.com.au